Published in final edited form as:
AJNR Am J Neuroradiol. 2011 August ; 32(7): 1280–1285. doi:10.3174/ajnr.A2540.

Clinical correlates of white matter perfusion changes in Sturge-Weber syndrome: A dynamic MR perfusion-weighted imaging study

Y Miao, **C Juhász**, **J Wu**, **B Tarabishy**, **Z Lang**, **ME Behen**, **Z Kou**, **Y Ye**, **HT Chugani**, and **J Hu**

Carman and Ann Adams Department of Pediatrics, Departments of Radiology and Neurology, Wayne State University School of Medicine, Detroit, MI, USA. Positron Emission Tomography Center, Children's Hospital of Michigan, Detroit, MI, USA. Department of Radiology, First Affiliated Hospital, Dalian Medical University, Dalian, Liaoning, China

Abstract

Background and Purpose—Low brain tissue perfusion due to abnormal venous drainage is thought to be a central mechanism of brain damage in Sturge-Weber syndrome (SWS). In the present study, high-resolution perfusion-weighted imaging (HR-PWI) was used to quantify white matter perfusion abnormalities and correlate these with brain atrophy and clinical variables.

Materials and Methods—Fourteen children (age: 0.8–10.0 years) with unilateral SWS underwent MRI examinations, including HR-PWI. Relative cerebral blood volume (rCBV), cerebral blood flow (rCBF) and mean transit time (MTT) in the affected white matter (WM) and in contralateral homotopic WM were measured. Asymmetry index (AI) for each perfusion parameter was correlated with age, brain atrophy, motor and seizure variables as well as IQ.

Results—Increased perfusion was seen in the affected hemisphere in 5 children and decreased perfusion in 9. Brain atrophy was more severe in the low-perfusion group ($p=0.01$) and was related to both CBF-AI and CBV-AI ($r = -0.69$, $p = 0.007$; $r = -0.64$, $p = 0.014$, respectively). Older children had lower CBV values on the affected side ($r = -0.62$, $p = 0.02$). Longer duration of epilepsy was related to lower CBF (more negative CBF-AI, $r=-0.58$, $p=0.03$) and low CBV ($r=-0.55$, $p=0.04$) on the affected side. Lower perfusion was associated with more frequent seizures (rCBF-AI: $r=-0.56$, $p=0.04$; rCBV-AI: $r=-0.63$, $p=0.02$).

Conclusion—Increased perfusion in the affected cerebral WM may indicate an early stage of SWS without severe brain atrophy. Decreased perfusion is associated with frequent seizures, long duration of epilepsy and brain atrophy.

Keywords

Sturge-Weber syndrome; MRI; perfusion; white matter; epilepsy

---

As a sporadic neurocutaneous disorder, Sturge-Weber syndrome (SWS) is classically characterized by a facial port-wine stain in the trigeminal nerve distribution, a leptomeningeal angioma and ocular abnormalities [1]. Progressive neurologic symptoms, including seizures, visual field defects, and hemiparesis, are often present in children with SWS, and are likely the result of hypoxia-induced cortical injury [2]. In contrast to the prominent pathological abnormalities in the cortex, including astrogliosis, atrophy and perivascular calcifications, the white matter (WM) shows relatively less structural abnormality on conventional MR imaging. Nevertheless, recent MR studies have recognized that structural changes in WM may play a major role in the clinical manifestations of SWS, such as cognitive impairment [3–6].

Abnormal cortical drainage and venous stasis result from an anomalous venous plexus over the cerebral surface in patients with SWS, leading to impaired cortical perfusion and ischemia, further aggravated by repetitive and progressively worsening seizures [2]. Nevertheless, it is unclear whether abnormal blood perfusion in the affected WM directly contributes to the clinical features of SWS. Previous functional neuroimaging, such as positron emission tomography (PET) and single photon emission computed tomography (SPECT) studies have found that blood flow deficit in the affected cortical regions was common in SWS, probably contributing to neurologic impairment [7–9]. Recent dynamic contrast enhanced MR perfusion weighted imaging (PWI) studies have also shown similar results [10–12]. In addition, a few patients have been reported to show *increased* blood flow in the affected cortex as detected by PWI or SPECT. Those patients typically had recent seizure onset [7, 13]. However, little research has focused on the hemodynamics in WM and its relation to the clinical features of SWS. In the present study, we combined PWI and conventional MR imaging to quantify WM perfusion in a prospectively recruited group of children with unilateral SWS. Furthermore, we paid particularly close attention to the correlation between perfusion parameters in WM and some putative impacting factors, including age, brain atrophy, and seizure variables, as well as the potential relation between WM perfusion status and motor as well as cognitive functions.

Materials and Methods

Subjects

In this study, data of 14 children (8 girls and 6 boys; age, 0.8–10.0 years; median age, 4.0 years) with unilateral SWS were analyzed, selected from 45 children recruited prospectively for a clinical and neuroimaging study of children with SWS between 2003 and 2010. The present study was based on the following inclusion criteria [5]: (1) diagnosis of SWS with unilateral brain involvement based on clinical and imaging features (conventional MRI as well as FDG PET, performed within 24 hours of the MRI studies) and (2) the availability of good quality PWI images. Patients were excluded if they had bilateral brain involvement, since an unaffected hemisphere must be present in order to make a meaningful comparison between sides on PWI. Of the 14 children, 13 had a history of seizures, and 7 suffered from hemiparesis of varying degrees and extent. Table 1 shows the clinical data, including age at MR examination (A_{mr}), age at first seizure (A_{sz}), average seizure frequency, duration of epilepsy and full scale IQ score.

Additionally, 10 healthy adults (5 males and 5 females; age, 22–47 years; median age, 34 years) were recruited as controls to establish normal perfusion parameter asymmetries between hemispheres. Exclusion criteria for this group included a history of a neurological or psychiatric condition, head trauma with loss of consciousness for more than five minutes, a habit of drug or alcohol abuse, brain surgery, as well as focal hyperintensity in the brain on T2-weighted images. The study was approved by the Wayne State University Human Investigation Committee, and informed consent of the parent or legal guardian was obtained.

MR imaging protocol

All children with SWS underwent an MRI examination using a Sonata 1.5 T MR scanner (Siemens, Erlangen, Germany) with a standard head coil. Patients younger than 7 years of age were sedated with pentobarbital (3 mg/kg) followed by fentanyl (1μg/kg). The MRI protocol included an axial 3D gradient-echo T1-weighted acquisition (TR=20 ms; TE=5.6 ms; flip angle=25°; voxel size=1.0×0.5×2.0 mm^3), an axial T2-weighted turbo spin-echo acquisition (TR=5020 ms; TE=106 ms; voxel size=1.0×1.0×6.0 mm^3), susceptibility weighted imaging (SWI), followed by dynamic contrast enhanced high-resolution MR perfusion-weighted imaging (HR-PWI) and a postgadolinium T1-weighted acquisition

(using the same imaging parameters as the first T1 weighted acquisition) and in all patients. The HR-PWI data were obtained using a two-dimensional gradient echo EPI sequence with TR = 2200 ms, TE = 98ms, flip angle = 60°, slice thickness = 4 mm. The field of view (FOV) was 256 mm × 256 mm and matrix was 512×512. The scan was run 50 times. The contrast agent gadolinium-DTPA (Magnevist, Berlex, USA) was bolus injected via a peripheral vein on one of the hands by a power injector (Medrad, Spectris MR injection system, USA) with a dose of 0.1 mmol/kg of body weight at a rate of 2 ml/sec. On PWI, a smaller voxel size of $0.5\times0.5\times4.0\ mm^3$, as compared to those published previously [10–12], was obtained to improve the ability of detecting subtle structures in cerebral parenchyma; therefore, the PWI method used here is termed high-resolution. The 10 control subjects also underwent HR-PWI with the same protocol.

MR data processing

Brain atrophy estimation—All acquired datasets were transferred to a PC workstation for postprocessing using a software developed in-house (Signal Process in Neuroimaging, SPIN [14,15]). The affected hemisphere was defined according to characteristic findings including leptomeningeal angioma and/or transmedullary veins as well as enlarged venous plexus on the contrast enhanced T1WI. T2WI images were used to measure the degree of brain atrophy because of its superior image contrast. Two neuroradiologists manually traced the areas of the affected hemisphere on T2WI in all selected slices (but a minimum of 3 consecutive slices) with vascular involvement as evidenced by contrast enhanced-T1WI. All slices showing involvement with abnormal vessels on contrast enhanced-T1WI were regarded as regions to be measured.

A hemispheric region of interest (ROI) was drawn along the surface of cortex and midline structures. The ROI included all cortex, WM and ventricle in a hemisphere in a slice. In the same way, contralateral hemispheric areas were also manually delineated in all affected slices. Moreover, the ipsilateral (affected) and contralateral hemispheric volumes were respectively obtained by calculating the sum of all affected slices. Brain atrophy asymmetry indices (BA-AI) were calculated by formula 1 [16]:

$$BA-AI=(\text{ipsilateral volume}-\text{contralateral volume})/([\text{ipsilateral volume}+\text{contralateral volume}]/2) \quad \text{Formula 1}$$

PWI analysis—Aseries of perfusion parameter maps were post-processed from MR perfusion raw data based on tracer kinetic methods [17], including regional cerebral blood volume (rCBV), regional cerebral blood flow (rCBF), and mean transit time (MTT), in SPIN software. Among these indices, rCBF values more directly and specifically reflect the blood flow status in the brain tissue. As a result, the rCBF map was chosen for comparing the cerebral perfusion between the two (affected vs. unaffected) hemispheres. rCBF, rCBV and rMTT values in the affected WM, defined by the presence of abnormally enhancing vessels and/or leptomeningeal venous angiomatosis, and contralateral homotopic WM were manually measured by two neuroradiologists. Three ROIs, 20–40 voxels in size, were placed on every slice in the affected and contralateral WM. On the CBF map, vessels and cortex are colored red and green respectively, while WM has a blue color, allowing for accurate placement of ROIs over WM, while also avoiding inclusion of vessels, cortex and ventricle, as shown on figure 1. Perfusion parameters were measured in all affected regions based on abnormal features on contrast-T1WI, including leptomeningeal angioma and/or dilated transmedullary veins, the very same features used to define involvement when calculating brain atrophy ratios as described above. The final values quoted were the mean of the measurements in all affected slices, yielding hemispheric perfusion parameter asymmetry indices (AI), calculated based on formula 2.

$$\begin{aligned} CBF-AI_s&=(CBFI-CBFC)/((CBFI+CBFC)/2);\\ CBV-AI_s&=(CBVI-CBVC)/((CBVI+CBVC)/2);\\ MTT-AI_s&=(MTTI-MTTC)/((MTTI+MTTC)/2). \end{aligned} \quad \text{Formula 2}$$

CBF-AI_s, CBV-AI_s and MTT-AI_s are the asymmetry indices of cerebral blood flow (CBF), cerebral blood volume (CBV) and mean transit time (MTT) in SWS patients; CBFI, CBVI and MTTI indicate the CBF, CBV and MTT values in WM ipsilateral to the angioma; CBFC, CBVC and MTTC are the perfusion values in the contralateral hemisphere, measured in homotopic regions.

Among the control group, the same three perfusion parameters were also measured in bilateral frontal, parietal, temporal and occipital WM. The ROIs were placed in deep frontal WM, posterior centrum semiovale, optic radiations and WM adjacent to temporal horn of the lateral ventricle. ROIs were 20–40 voxels in size. Measurements were made slice-by-slice by placing ROIs on WM in the areas described above. The mean and standard deviation (SD) of perfusion asymmetry indices (CBF-AI_c, CBV-AI_c and MTT-AI_c) were calculated, thus creating a reference to determine the perfusion contrast between hemispheres in SWS cases, according to formula 3.

$$\begin{aligned} CBF-AI_c&=(CBFR-CBFL)/((CBFR+CBFL)/2);\\ CBV-AI_c&=(CBVR-CBVL)/((CBVR+CBVL)/2);\\ MTT-AI_c&=(MTTR-MTTL)/((MTTR+MTTL)/2). \end{aligned} \quad \text{Formula 3}$$

CBF-AI_c, CBV-AI_c and MTT-AI_c are the asymmetry indices of cerebral blood flow (CBF), cerebral blood volume (CBV) and mean transit time (MTT) between hemispheres in controls; CBFR, CBVR and MTTR indicate the CBF, CBV and MTT values in the right white matter; CBFL CBVL and MTL are the perfusion values in the left hemisphere, measured in homotopic regions.

Assessment of Cognitive Functions

All children received a comprehensive neuropsychological assessment within 1 day of the MRI studies, administered by a pediatric neuropsychologist. Neuropsychological testing for global intellectual functioning (IQ) was performed in the morning, before sedation for imaging, using previously detailed protocols in all children above 18 months of age (n=13) [3, 5].

Seizure frequency score

Since seizure frequency could not be determined with exact accuracy, a seizure frequency score was calculated based on a scoring system proposed by Engel et al [18]. We have used a simplified version of this scoring system according to a 5-point scale as follows: 1: ≤1 seizure per year; 2: 2–11 seizures per year; 3: 1–3 seizure(s) per month; 4: 1–6 seizure(s) per week; 5: ≥1 seizure(s) per day.

Statistical analysis

Reliability of measurements was first investigated with a desired correlation coefficient value of greater than 0.90 [19] by Single Measure Intraclass Correlation after the rCBF, rCBV, rMTT and BA-AI values had been measured twice by two neuroradiologists for all the subjects. Group comparisons of perfusion variables and AIs were performed by Mann-Whitney U test using SPSS (Release 16.0; SPSS, Chicago, IL), due to the non-normality distribution occurring in part of the data. Relationships between these perfusion values and

age at MRI examination (A_{mr}), BA-AI, seizure frequency, duration of epilepsy, age at epilepsy onset (A_{sz}) and IQ scores were determined by non-parametric Spearman's rank correlation. All statistics was performed with a 0.05 level of significance.

Results

Intraclass and interclass reliability of hemispheric atrophy and perfusion measurements

The intraclass and interclass reliability of rCBF, rCBV, rMTT in the SWS cases and controls and BA-AI values in the SWS subjects were beyond our target value of 0.90, varying from 0.93 to 0.98 and 0.94 to 0.97 respectively.

Perfusion asymmetries: high- and low-perfusion in the affected hemisphere

Among the control group, the mean and SD of CBF-AI, CBV-AI and MTT-AI were − 0.004 ±0.006, 0.009±0.014 and 0.008±0.008, respectively. A cut-off of 2 SDs above and below the mean for CBF-AI (0.008, −0.016; i.e., less than 2% asymmetries in normal brain) was defined as the normal range. CBF-AI values falling outside this range for the SWS group were regarded as abnormal.

In the SWS group, CBF-AI_s varied between −0.82 and +0.39, while CBV- AI_s varied between −0.67 and +0.69. All CBF-AI_s values were considerably outside the normal range (the smallest AI was −0.12, consistent with a 12% asymmetry), and patients were divided into two subgroups according to their CBF-AI_s values: A relative low perfusion (rLP) group (negative CBF-AI_s, indicating abnormally low perfusion on the angioma side; n=9; see an example on figure 1) and a relative high perfusion (rHP) group (positive CBF-AI_s, increased perfusion on the angioma side; n=5; figure 2). Detailed results are listed in table 2. It should be noted that 4 of the 5 children with high perfusion had a history of seizures, but all 4 were free of clinical seizures for at least 4 months before the MRI scan.

BA-AI in the rLP group was significantly lower (mean: −0.15, i.e., an average of 15% volume decrease) than in the rHP group (−0.04; p=0.01), indicating more severe atrophy in the affected brain regions of the rLP group on the side affected by the venous angioma. In contrast, there was no significant difference in age (A_{mr}) or IQ between the groups, although there was a moderate trend for lower age in the rHP group, as compared to the age of children in the rLP group (mean age = 3.6 vs. 5.3 years, Z=−1.41, p = 0.16).

Correlation between perfusion status and age, atrophy, hemiparesis and IQ

A significant negative correlation was found between the age at MRI examination and CBV value on the affected side (r = −0.62, p = 0.02). There was a trend towards a negative correlation with CBF-AI_s (r=−0.50, p=0.065). BA-AI values also demonstrated a significant positive correlation with CBF-AI_s as well as CBV-AI_s (r = 0.69, p = 0.007; r = 0.64, p = 0.014, respectively). Patients with hemiparesis (n=7) had more severe brain atrophy AIs than those with no paresis (BA-AI: 0.17±0.10 vs. 0.05±0.06, respectively); however, perfusion variables were not different between the two subgroups (p>0.1 in all comparisons). Also, there was no relation between perfusion values/asymmetries and IQ of children (p>0.6 in all comparisons), although all 3 patients with IQ <70 (>2SD below normal mean) had low CBF-AI_S values (ranging from −0.82 to −0.28).

Relation between perfusion status and seizure variables

Low CBF-AI values (r=−0.58, p=0.03) and decreased ipsilateral CBV (r=−0.55, p=0.04) were found to correlate with a longer duration of epilepsy. No significant correlation was found between MTTs, MTT-AIs and duration of epilepsy. Both rCBF and rCBV asymmetries (but not MTT parameters) also showed an inverse correlation with seizure

frequency scores ($r=-0.56$, $p=0.04$ and $r=-0.63$, $p=0.02$, respectively). Duration of epilepsy and seizure frequency did not correlate with each other ($p=0.60$). Age at epilepsy onset (A_{sz}) did not correlate with any perfusion parameter ($p>0.2$ in all correlations).

Discussion

Our study provides a new perspective on quantitative relationships among brain white matter (WM) perfusion, brain atrophy and seizure severity in patients with Sturge-Weber syndrome. Specifically, we demonstrated that: a) Increased blood flow in the affected hemisphere appears to be a relatively common phenomenon in children with SWS, found in more than 1/3 of the present patient sample, especially in younger children; b) WM hypoperfusion in the affected hemisphere is associated with a long history of epilepsy and more severe brain atrophy, suggesting a progressive deterioration of perfusion status over time, leading to brain tissue loss; and c) A significant relationship exists between seizure frequency and severity of white matter hypoperfusion, suggesting a link between low brain perfusion and chronic seizures in SWS. This is in contrast with the conventional notion that SWS pathology is mostly confined to gray matter or regions of anomalous venous drainage. Despite the relatively normal appearance on conventional MRI, our data shows the importance of WM perfusion in structural changes and seizure severity. Meanwhile, we could not demonstrate that white matter perfusion status was a robust predictor of cognitive functions or motor impairment. It should be noted, however, that most children in this study had relatively good cognitive functions, which made this statistical comparison less useful. Motor dysfunction is more likely related to localized abnormalities in white matter regions encompassing motor pathways, as suggested by diffusion tensor imaging studies [6].

The characteristic vascular malformation of SWS and its associated abnormalities have been well described in the literature and include a leptomeningeal angioma displacing normal superficial cortical veins, compensatory dilatation of the deep venous system, ipsilateral choroid plexus hypertrophy and subsequent development of atrophic and calcified cerebral cortex due to neuronal loss and astrogliosis [1, 2, 20–22]. Although MRI signs of ‘accelerated myelination’ have been described in infants with SWS [23], only a few recent MRI studies focused on the significance of white matter pathology using quantitative volumetry [3] or water diffusion measurements [4–6]. MRI studies of cerebral perfusion performed in small groups of SWS patients demonstrated mostly decreased perfusion in regions with meningeal enhancement [11, 12]; additional perfusion defects were seen in areas of deep venous abnormalities. Based on histological studies, the cortical blood flow reduction was speculated to be secondary to the venous stasis and hypertension due to malformed, cortical vessels as well as venous thrombosis [1, 2, 24, 25]. Nevertheless, a SPECT study found *hyper*perfused cortex in some infants with SWS even before their first seizures [7]. A more recent MRI study also reported increased relative cerebral blood flow and volume of the affected cerebral tissue in 2 children with SWS and recent onset seizures [13]. Possible causes of increased perfusion in their studies included altered hemodynamics due to recent seizures; however, the exact mechanism leading to blood flow increases remained unclear. In our study, children with relative hyperperfusion in the affected WM had no recent seizures but were slightly younger and had milder brain atrophy, while those with decreased perfusion had a more advanced disease with long duration of epilepsy and atrophy. This suggests that hyperperfusion is an interictal phenomenon and may represent a relatively early stage of pathology possibly indicating ongoing hypoxic injury. Increased cerebral blood flow on PWI has been indeed reported in neonates with hypoxic-ischemic encephalopathy [26]; changes involved the white matter in some cases and were hypothesized to represent ongoing injury in reperfusion areas with abnormal cerebral autoregulation. Transient increase of glucose metabolism, also described in young children with hypoxic damage (due to both SWS and perinatal hypoxia), may be a metabolic aspect

of the same phenomenon, possibly indicating hypoxia-induced, glutamatergic excitotoxic injury leading to subsequent tissue loss and hypometabolism [27–31].

Our previous study showed a significant negative correlation between hemispheric white matter volume and age in children with SWS [3]. Hypoxic injury due to impaired venous drainage of the affected hemisphere was considered as the putative mechanism causing early WM abnormalities [32]. The present PWI study provides further evidence for WM injury at the perfusion level with relation to age as well as brain atrophy. Decreased blood flow in brain tissue corresponding to the vascular abnormalities over time may aggravate the extent of hypoxic injury leading to progressive neuronal death, astrogliosis, and atrophy. Since blood flow changes can occur prior to structural abnormalities in SWS [10, 11], early perfusion abnormality may be a useful imaging marker to indicate imminent white matter damage.

The results also have implications regarding the pathomechanism of seizures in SWS. The association of long duration of epilepsy and high seizure frequency with severe hypoperfusion suggests that chronic hypoperfusion and tissue hypoxia may play a role in seizure generation in SWS. On the other hand, frequent seizures may contribute to brain ischemia and disease progression. The findings suggest that improved tissue perfusion may lead to better seizure control, while lower seizure frequency may also prevent progressive ischemic damage. Longitudinal studies could further elucidate the exact causative relationship between brain perfusion status and seizure severity in SWS.

Several methodological issues should be considered when interpreting our data. First, perfusion measurements may be affected to some extent by brain atrophy and cortical calcification in the affected hemisphere. This effect was largely diminished by carefully placing multiple ROIs in WM regions, avoiding cortex (where calcification is most likely and artifacts from blood flow changes from overlying angioma may confound accurate perfusion measurements from brain tissue) and also large vessels, so that the measured data reflect tissue perfusion. Moreover, calculation of brain atrophy asymmetry (BA-AI) included both gray matter and white matter volume. It remains to be determined whether perfusion abnormalities affect gray and white matter volumes differentially. Also, our control group included adults, and we relied on asymmetry measurements to define abnormal decreases and increases in the affected hemisphere. This approach appears to be valid, as it does not rely on measurement of absolute perfusion values, which undergo non-linear changes during childhood (an early increase during the first 2–3 years of life and a gradual decrease during adolescence [33–34]).

Conclusions

MR perfusion-weighted imaging of the affected cerebral white matter indicates dynamic perfusion abnormalities in children with SWS: increased perfusion in mostly younger patients may represent a transient phenomenon, before severe brain atrophy occurs in the affected brain regions. Decreased perfusion is associated with high seizure frequency, long epilepsy duration and brain atrophy, suggesting a detrimental effect of chronic seizures on brain structure and function. MR PWI is a helpful technique to quantitatively evaluate blood flow abnormalities at different stages of evolution of SWS.

Acknowledgments

We are grateful to Yang Xuan BS for his technical support in the MRI acquisition. We also thank Majid Khalaf MD, Anne Deboard RN and Jane Cornett RN for their assistance in sedation. We thank the Sturge-Weber Foundation for referring patients to us. We are also grateful to the families and children who participated in the study.

Abbreviation key

SWS	Sturge-Weber syndrome
WM	white matter
CBV	cerebral blood volume
CBF	cerebral blood flow
MTT	mean transit time
AI	asymmetry index

References

1. Comi AM. Advances in Sturge-Weber syndrome. Curr Opin Neurol. 2006; 19(2):124–128. [PubMed: 16538084]
2. Comi AM. Pathophysiology of Sturge-Weber Syndrome. J Child Neurol. 2003; 18(8):509–516. [PubMed: 13677575]
3. Juhasz C, Lai Ch, Behen ME, et al. White matter volume as a major predictor of cognitive function in Sturge-Weber Syndrome. Arch Neurol. 2007; 64(8):1169–1174. [PubMed: 17698708]
4. Deary IJ, Bastin ME, Pattie A, et al. White matter integrity and cognition in childhood and old age. Neurology. 2006; 66 (4):505–512. [PubMed: 16505302]
5. Juhasz C, Haacke EM, Hu J, et al. Multimodality imaging of cortical and white matter abnormalities in Sturge-Weber Syndrome. AJNR Am J Neuroradiol. 2007; 28(5):900–906. [PubMed: 17494666]
6. Alkonyi B, Govindan RM, Chugani HT, Behen ME, Jeong JW, Juhász C. Focal white matter abnormalities related to neurocognitive dysfunction: An objective diffusion tensor imaging study of children with Sturge-Weber syndrome. Pediatr Res. 2010 Sept 17. (Epub ahead of print).
7. Pinton F, Chiron C, Enjolras O, Motte J, Syrota A, Dulac O. Early single photon emission computed tomography in Sturge-Weber syndrome. J Neurol Neurosurg Psychiatry. 1997; 63(5):616–621. [PubMed: 9408103]
8. Duncan DB, Herholz K, Pietrzyk U, Heiss WD. Regional cerebral blood flow and metabolism in Sturge-Weber disease. Clin Nucl Med. 1995; 20(6):522–523. [PubMed: 7648737]
9. Maria BL, Neufeld JA, Rosainz LC, Ben-David K, Drane WE, Quisling RG, Hamed LM. High prevalence of bihemispheric structural and functional defects in Sturge-Weber syndrome. J Child Neurol. 1998; 13(12):595–605. [PubMed: 9881530]
10. Lin DD, Barker PB, Kraut MA, Comi A. Early Characteristics of Sturge-Weber Syndrome Shown by Perfusion MR Imaging and Proton MR Spectroscopic Imaging. AJNR Am J Neuroradiol. 2003; 24(9):1912–1915. [PubMed: 14561628]
11. Evans AL, Widjaja E, Connolly DJ, Griffiths PD. Cerebral perfusion abnormalities in children with Sturge-Weber Syndrome shown by dynamic contrast bolus magnetic resonance perfusion imaging. Pediatrics. 2006; 117(6):2119–2125. [PubMed: 16740855]
12. Lin DD, Barker PB, Hatfield LA, Comi AM. Dynamic MR Perfusion and Proton MR Spectroscopic Imaging in Sturge-Weber Syndrome: Correlation With Neurological Symptoms. J Magn Reson Imag. 2006; 24(2):274–281.
13. Oguz KK, Senturk S, Ozturk A, Anlar B, Topcu M, Cila A. Impact of recent seizures on cerebral blood flow in patients with sturge-weber syndrome: study of 2 cases. J Child Neurol. 2007; 22(5): 617–620. [PubMed: 17690070]
14. Haacke EM, Ayaz M, Khan A, et al. Establishing a baseline phase behavior in magnetic resonance imaging to determine normal vs. abnormal iron content in the brain. J Magn Reson Imag. 2007; 26(2):256–264.
15. Haacke EM, Mittal S, Wu Z, et al. Susceptibility-weighted imaging: technical aspects and clinical applications, part 1. AJNR Am J Neuroradiol. 2009; 30(1):19–30. [PubMed: 19039041]

16. Kelley TM, Hatfield LA, Lin DD, Comi AM. Quantitative Analysis of Cerebral Cortical Atrophy and Correlation With Clinical Severity in Unilateral Sturge-Weber Syndrome. J Child Neurol. 2005; 20(11):867–870. [PubMed: 16417855]

17. Ostergaard L, Weisskoff RM, Chesler DA, Gyldensted C, Rosen BR. High resolution measurement of cerebral blood flow using intravascular tracer bolus passages. Part I: Mathematical approach and statistical analysis. Magn Reson Med. 1996; 36(5):715–725. [PubMed: 8916022]

18. Engel, J., Jr; Van Ness, PC.; Rasmussen, TB.; Ojemann, LM. Outcome with respect to epileptic seizures. In: Engel, J., Jr, editor. Surgical treatment of the epilepsies. 2. Raven Press; NY: 1993. p. 609-621.

19. Shrout PE, Fleiss JL. Intraclass correlations: uses in assessing raters reliability. Psychol Bull. 1979; 86(2):420–428. [PubMed: 18839484]

20. Norman MG, Schoene WC. The ultrastructure of Sturge-Weber disease. Acta Neuropathol (Berl). 1977; 37(3):199–205. [PubMed: 855646]

21. Di Trapani G, Di Rocco C, Abbamondi AL, et al. Light microscopy and ultrastructural studies of Sturge-Weber disease. Childs Brain. 1982; 9(1):23–36. [PubMed: 6460599]

22. Simonati A, Colamaria V, Bricolo A, et al. Microgyria associated with Sturge-Weber angiomatosis. Childs Nerv Syst. 1994; 10(6):392–395. [PubMed: 7842427]

23. Adamsbaum C, Pinton F, Rolland Y, Chiron C, Dulac O, Kalifa G. Accelerated myelination in early Sturge-Weber syndrome: MRI-SPECT correlations. Pediatr Radiol. 1996; 26(11):759–762. [PubMed: 8929371]

24. Prayson RA, Grewal ID, McMahon JT, et al. Leukocyte adhesion molecules and x-ray energy dispersive spectroscopy in Sturge-Weber disease. Pediatr Neurol. 1996; 15(4):332–336. [PubMed: 8972534]

25. Cunha e Sá M, Barroso CP, Caldas MC, Edvinsson L, Gulbenkian S. Innervation pattern of malformative cortical vessels in Sturge-Weber disease: an histochemical, immunohistochemical, and ultrastructural study. Neurosurgery. 1997; 41(4):872–876. [PubMed: 9316049]

26. Wintermark P, Moessinger AC, Gudinchet F, Meuli R. Perfusion-weighted magnetic resonance imaging patterns of hypoxic-ischemic encephalopathy in term neonates. J Magn Reson Imaging. 2008; 28(4):1019–1025. [PubMed: 18821602]

27. Chugani HT, Mazziotta JC, Phelps ME. Sturge-Weber syndrome: a study of cerebral glucose utilization with positron emission tomography. J Pediatr. 1989; 114(2):244–253. [PubMed: 2783735]

28. Pu Y, Li QF, Zeng CM, et al. Increased detectability of alpha brain glutamate/glutamine in neonatal hypoxic-ischemic encephalopathy. AJNR Am J Neuroradiol. 2000; 21(1):203–212. [PubMed: 10669252]

29. Hagberg H, Thornberg E, Blennow M, Kjellmer I, Lagercrantz H, Thiringer K, Hamberger A, Sandberg M. Excitatory amino acids in the cerebrospinal fluid of asphyxiated infants: relationship to hypoxic-ischemic encephalopathy. Acta Paediatr. 1993; 82(11):925–929. [PubMed: 7906573]

30. Blennow M, Ingvar M, Lagercrantz H, Stone-Elander S, Eriksson L, Forssberg H, Ericson K, Flodmark O. Early [^{18}F]FDG positron emission tomography in infants with hypoxic-ischaemic encephalopathy shows hypermetabolism during the postasphyctic period. Acta Paediatr. 1995; 84(11):1289–1295. [PubMed: 8580629]

31. Batista CE, Chugani HT, Juhasz C, Behen ME, Shankaran S. Transient hypermetabolism of the basal ganglia following perinatal hypoxia. Pediatr Neurol. 2007; 36(5):330–333. [PubMed: 17509466]

32. Pfund Z, Kagawa K, Juhasz C, et al. Quantitative analysis of gray- and white matter volumes and glucose metabolism in Sturge-Weber syndrome. J Child Neurol. 2003; 18(2):119–126. [PubMed: 12693779]

33. Biagi L, Abbruzzese A, Bianchi MC, Alsop DC, Del Guerra A, Tosetti M. Age dependence of cerebral perfusion assessed by magnetic resonance continuous arterial spin labeling. J Magn Reson Imaging. 2007; 25(4):696–702. [PubMed: 17279531]

34. Bjørnerud A, Emblem KE. A fully automated method for quantitative cerebral hemodynamic analysis using DSC-MRI. J Cereb Blood Flow Metab. 2010; 30(5):1066–1078. [PubMed: 20087370]

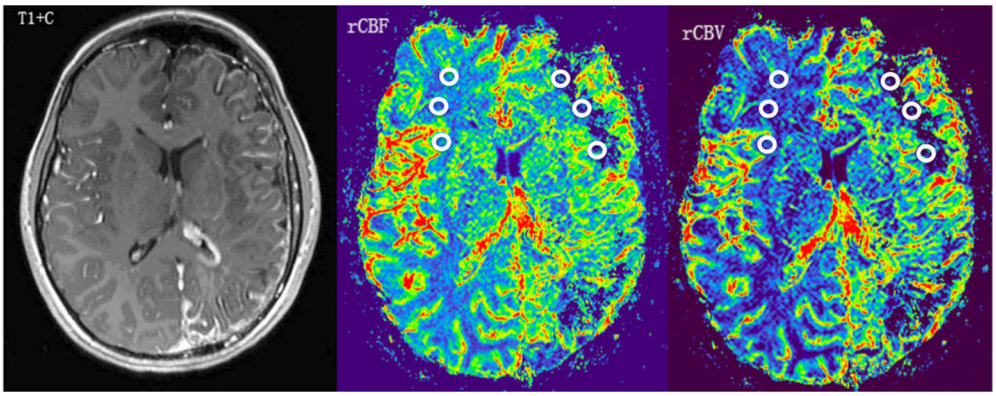

Figure 1.

A 10-year-old girl with developmental delay (IQ=55) and monthly seizures (patient 3 in tables 1 and 2). Contrast-enhanced T1-weighted image (T1+C) shows left hemisphere volume loss and characteristic leptomeningeal enhancement in the same region, as well as a prominent left choroid plexus. PWI demonstrates decreased rCBF and rCBV (CBF-AI_s= −0.67, CBV-AI_s =−0.52) in the left frontal and occipital white matter regions, underlying the leptomeningeal angiomatosis. Regions of interest placed on the affected left frontal white matter and contralateral homotopic region are demonstrated.

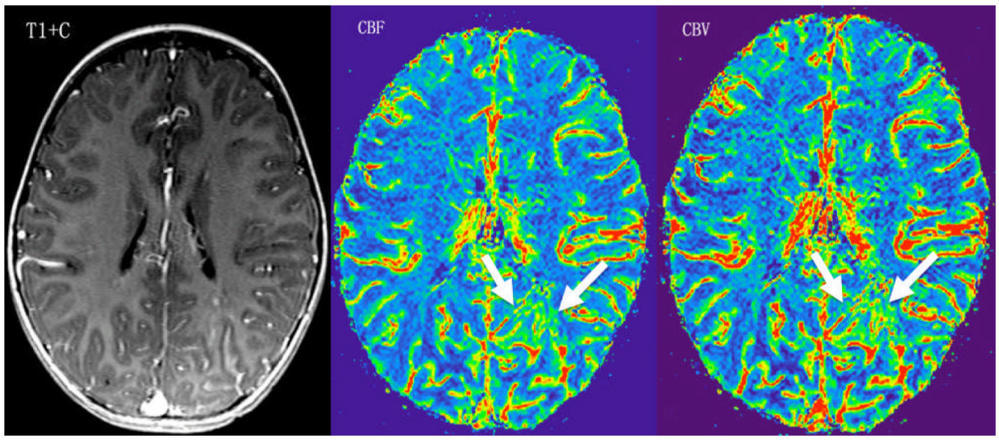

Figure 2.
A 2.0-year-old girl with normal cognitive development (IQ=105) and no seizures. Contrast-enhanced T1-weighted image (T1+C) shows leptomeningeal enhancement in the left occipital lobe. PWI demonstrates increased white matter rCBF and rCBV (CBF-AI=0.26, CBV-AI=0.24) in the involved région (arrows).

Table 1

Clinical data of all children with Sturge-Weber syndrome

patient	gender	age (years) at MRI	age (years) at first seizure	seizure frequency	last seizure before MRI	IQ	hemiparesis	antiepileptic drug
1	M	7.0	0.5	>10/day	2 hours	47	yes	VPA, LEV
2	F	2.0	0.1	1/year	>1 year	55	yes	CBZ, PHB, CLOB
3	F	10.0	0.2	monthly	1 year	55	yes	LAM
4	F	5.0	0.5	<1/year	6 months	117	no	PHB
5	M	5.0	5.0	monthly	12 hours	99	no	PHT, LEV
6	M	1.8	0.7	10/mo	2 days	105	no	PHB, LEV, OXC
7	F	0.8	0.2	few/month	1 month	---	yes	PHB, OXC, LEV
8	M	4.0	3.5	weekly	10 days	110	no	OXC
9	M	9.0	0.6	1/year	9 months	93	yes	CBZ
10	F	1.6	0.6	few/year	6 months	71	yes	LEV, VPA
11	M	1.8	1.6	few/year	4 months	92	no	LEV
12	F	2.0	---	0	---	105	no	none
13	F	4.0	2.0	<1/year	>1 year	102	no	LAM
14	F	4.0	0.1	<1/year	>1 year	91	yes	OXC

VPA=valproate, OXC=oxcarbazepine, LEV=levetiracetam, CBZ=carbamazepine, PHT=phenytoin, PHB=phenobarbital, CLOB=clobazam; IQ was not assessed for the child (#7) below 1 year of age

Table 2

Brain atrophy, rCBF, rCBV and rMTT values measured in the white matter ipsi- and contralateral to the angioma

Perfusion Group	Location of angioma	BA-AI	rCBF			rCBV			rMTT		
			CBF Ipsi	CBF Cont	CBF-AI$_S$	CBV Ipsi	CBV Cont	CBV-AI$_S$	MTT Ipsi	MTT Cont	MTT-AI$_S$
1	left FPO	-0.17	16.65	39.67	-0.82	2.33	4.65	-0.67	4.58	7.17	-0.44
1	left FPTO	-0.35	44.49	58.84	-0.28	4.77	5.41	-0.13	5.65	5.75	-0.02
1	left FTPO	-0.23	29.04	58.42	-0.67	3.33	5.68	-0.52	3.46	5.95	-0.53
1	left TO	-0.13	22.16	32.87	-0.39	3.49	4.88	-0.33	7.48	9.02	-0.19
1	right PO	-0.05	35.08	41.26	-0.16	3.96	3.87	0.02	7.46	5.67	0.27
1	left PTO	-0.13	30.77	49.03	-0.46	2.31	2.93	-0.24	1.22	3.63	-0.99
1	right FPTO	-0.21	64.57	77.80	-0.19	5.82	6.27	-0.07	5.57	4.99	0.11
1	left PO	-0.03	50.24	56.56	-0.12	4.88	5.31	-0.08	5.91	5.71	0.04
1	left P	-0.07	20.17	25.14	-0.22	1.08	1.03	0.05	3.19	2.64	0.19
2	right FPTO	-0.11	63.05	42.52	0.39	6.11	2.97	0.69	5.83	4.36	0.29
2	right PTO	-0.04	20.40	14.70	0.32	6.00	4.38	0.31	17.64	17.57	0.00
2	left PTO	0.01	19.66	15.11	0.26	5.73	4.52	0.24	17.85	18.14	-0.02
2	left P	0.01	84.04	62.13	0.30	6.92	4.56	0.41	5.18	4.60	0.12
2	left FP	-0.07	55.03	41.02	0.29	5.21	3.58	0.37	6.00	5.64	0.06
P value		0.01	0.46	0.32	<0.001	0.01	0.21	<0.001	0.10	0.74	0.21

Note: P values were calculated by comparison of variables (using Mann-Whitney U-test) between low-perfusion (group 1) and high-perfusion (group 2) subgroups, based on CBF asymmetries comparing sides ipsi- vs. contralateral to the angioma.

Abbreviations: BA-AI: brain atrophy asymmetry index; CBF: cerebral blood flow; CBV: cerebral blood volume; MTT: mean transit time; Ipsi: ipsilateral, Cont: contralateral (to angioma); AI = asymmetry index